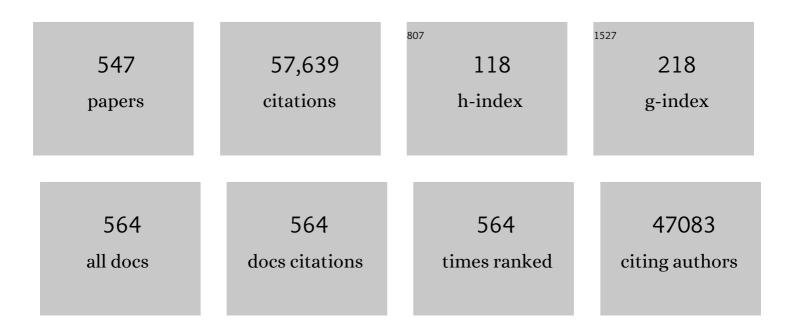


List of Publications by Year in descending order

Source: https://exaly.com/author-pdf/6148142/publications.pdf Version: 2024-02-01



lu lu

#	Article	IF	CITATIONS
1	Machine learning of metal-ceramic wettability. Journal of Materiomics, 2022, 8, 195-203.	2.8	6
2	EML webinar overview: Elastic Strain Engineering for unprecedented properties. Extreme Mechanics Letters, 2022, 54, 101430.	2.0	5
3	Electrochemically stable lithium-ion and electron insulators (LEIs) for solid-state batteries. Nano Research, 2022, 15, 1213-1220.	5.8	4
4	Deep neural network battery life and voltage prediction by using data of one cycle only. Applied Energy, 2022, 306, 118134.	5.1	57
5	Effects of Elemental Modulation on Phase Purity and Electrochemical Properties of Coâ€free Highâ€Entropy Spinel Oxide Anodes for Lithiumâ€ion Batteries. Advanced Functional Materials, 2022, 32, .	7.8	48
6	Machine learning in nuclear materials research. Current Opinion in Solid State and Materials Science, 2022, 26, 100975.	5.6	42
7	Learning constitutive relations of plasticity using neural networks and full-field data. Extreme Mechanics Letters, 2022, 52, 101645.	2.0	2
8	In situ TEM visualization of LiF nanosheet formation on the cathode-electrolyte interphase (CEI) in liquid-electrolyte lithium-ion batteries. Matter, 2022, 5, 1235-1250.	5.0	56
9	Rejuvenation of plasticity via deformation graining in magnesium. Nature Communications, 2022, 13, 1060.	5.8	26
10	Cryoâ€Electron Tomography of Highly Deformable and Adherent Solidâ€Electrolyte Interphase Exoskeleton in Liâ€Metal Batteries with Etherâ€Based Electrolyte. Advanced Materials, 2022, 34, e2108252.	11.1	20
11	Charging sustainable batteries. Nature Sustainability, 2022, 5, 176-178.	11.5	70
12	Evidence of fifth- and higher-order phonon scattering entropy of zone-center optical phonons. Physical Review B, 2022, 105, .	1.1	10
13	Synthesizing Functional Ceramic Powders for Solid Oxide Cells in Minutes through Thermal Shock. ACS Energy Letters, 2022, 7, 1223-1229.	8.8	6
14	Pressureless two-step sintering of ultrafine-grained refractory metals: Tungsten-rhenium and molybdenum. Journal of Materials Science and Technology, 2022, 126, 203-214.	5.6	13
15	Cryoâ€Electron Tomography of Highly Deformable and Adherent Solidâ€Electrolyte Interphase Exoskeleton in Liâ€Metal Batteries with Etherâ€Based Electrolyte (Adv. Mater. 13/2022). Advanced Materials, 2022, 34, .	11.1	2
16	TeaNet: Universal neural network interatomic potential inspired by iterative electronic relaxations. Computational Materials Science, 2022, 207, 111280.	1.4	21
17	Intelligent disassembly of electric-vehicle batteries: a forward-looking overview. Resources, Conservation and Recycling, 2022, 182, 106207.	5.3	41
18	Dislocationâ€Mediated Hydride Precipitation in Zirconium. Small, 2022, 18, e2105881.	5.2	4

#	Article	IF	CITATIONS
19	Healing of donor defect states in monolayer molybdenum disulfide using oxygen-incorporated chemical vapour deposition. Nature Electronics, 2022, 5, 28-36.	13.1	44
20	Revitalizing interface in protonic ceramic cells by acid etch. Nature, 2022, 604, 479-485.	13.7	132
21	Ultralong one-dimensional plastic zone created in aluminum underneath a nanoscale indent. Acta Materialia, 2022, 232, 117944.	3.8	12
22	Acidâ€inâ€Clay Electrolyte for Wideâ€Temperatureâ€Range and Longâ€Cycle Proton Batteries. Advanced Materials, 2022, 34, e2202063.	11.1	16
23	Enhanced mobility of cations and anions in the redox state: The polaronium mechanism. Acta Materialia, 2022, 232, 117941.	3.8	14
24	Anodic Shock-Triggered Exsolution of Metal Nanoparticles from Perovskite Oxide. Journal of the American Chemical Society, 2022, 144, 7657-7666.	6.6	15
25	Battery degradation prediction against uncertain future conditions with recurrent neural network enabled deep learning. Energy Storage Materials, 2022, 50, 139-151.	9.5	61
26	Abnormal nonlinear optical responses on the surface of topological materials. Npj Computational Materials, 2022, 8, .	3.5	6
27	Charge–Discharge Mechanism of Highâ€Entropy Coâ€Free Spinel Oxide Toward Li ⁺ Storage Examined Using Operando Quickâ€Scanning Xâ€Ray Absorption Spectroscopy. Advanced Science, 2022, 9, .	5.6	28
28	Generalized Wilson loop method for nonlinear light-matter interaction. Npj Quantum Materials, 2022, 7, .	1.8	10
29	Transverse and Longitudinal Degradations in Ceramic Solid Electrolytes. Chemistry of Materials, 2022, 34, 5749-5765.	3.2	20
30	An Unbalanced Battle in Excellence: Revealing Effect of Ni/Co Occupancy on Water Splitting and Oxygen Reduction Reactions in Triple onducting Oxides for Protonic Ceramic Electrochemical Cells. Small, 2022, 18, .	5.2	16
31	Nonlinear nonreciprocal photocurrents under phonon dressing. Physical Review B, 2022, 106, .	1.1	3
32	Electrospinningâ€Based Strategies for Battery Materials. Advanced Energy Materials, 2021, 11, 2000845.	10.2	169
33	Lithium Manganese Spinel Cathodes for Lithiumâ€lon Batteries. Advanced Energy Materials, 2021, 11, 2000997.	10.2	177
34	Ultraâ€Uniform Nanocrystalline Materials via Two‣tep Sintering. Advanced Functional Materials, 2021, 31, .	7.8	41
35	Coarse-grained reduced Mo Ti1â^'Nb2O7+ anodes for high-rate lithium-ion batteries. Energy Storage Materials, 2021, 34, 574-581.	9.5	13
36	Carbon nanotube (CNT) metal composites exhibit greatly reduced radiation damage. Acta Materialia, 2021, 203, 116483.	3.8	23

#	Article	IF	CITATIONS
37	Additive manufacturing for energy: A review. Applied Energy, 2021, 282, 116041.	5.1	146
38	Chemical and structural origin of hole states in yttria-stabilized zirconia. Acta Materialia, 2021, 203, 116487.	3.8	15
39	Achieving large uniform tensile elasticity in microfabricated diamond. Science, 2021, 371, 76-78.	6.0	95
40	Additive stabilization of SEI on graphite observed using cryo-electron microscopy. Energy and Environmental Science, 2021, 14, 4882-4889.	15.6	73
41	The impact of hydrogen valence on its bonding and transport in molten fluoride salts. Journal of Materials Chemistry A, 2021, 9, 1784-1794.	5.2	18
42	Analysis of SteraMist ionized hydrogen peroxide technology in the sterilization of N95 respirators and other PPE. Scientific Reports, 2021, 11, 2051.	1.6	34
43	Layer number dependent ferroelasticity in 2D Ruddlesden–Popper organic-inorganic hybrid perovskites. Nature Communications, 2021, 12, 1332.	5.8	28
44	Boosting photocatalytic hydrogen production from water by photothermally induced biphase systems. Nature Communications, 2021, 12, 1343.	5.8	209
45	Colossal switchable photocurrents in topological Janus transition metal dichalcogenides. Npj Computational Materials, 2021, 7, .	3.5	27
46	Interplay of Lithium Intercalation and Plating on a Single Graphite Particle. Joule, 2021, 5, 393-414.	11.7	168
47	Complex Structure of Molten NaCl–CrCl ₃ Salt: Cr–Cl Octahedral Network and Intermediate-Range Order. ACS Applied Energy Materials, 2021, 4, 3044-3056.	2.5	14
48	Porous Mixed Ionic Electronic Conductor Interlayers for Solid-State Batteries. Energy Material Advances, 2021, 2021, .	4.7	31
49	Effects of recoil spectra and electronic energy dissipation on defect survival in 3C-SiC. Materialia, 2021, 15, 101023.	1.3	7
50	Development of robust neural-network interatomic potential for molten salt. Cell Reports Physical Science, 2021, 2, 100359.	2.8	40
51	Reactive boride infusion stabilizes Ni-rich cathodes for lithium-ion batteries. Nature Energy, 2021, 6, 362-371.	19.8	274
52	Ultra-high-voltage Ni-rich layered cathodes in practical Li metal batteries enabled by a sulfonamide-based electrolyte. Nature Energy, 2021, 6, 495-505.	19.8	323
53	Hybrid diffusive-displacive helium outgassing in Cu/Nb multilayer composites. Scripta Materialia, 2021, 194, 113706.	2.6	10
54	Achieving room-temperature M2-phase VO2 nanowires for superior thermal actuation. Nano Research, 2021, 14, 4146-4153.	5.8	10

#	Article	IF	CITATIONS
55	Phase transitions in 2D materials. Nature Reviews Materials, 2021, 6, 829-846.	23.3	205
56	Terahertz Driven Reversible Topological Phase Transition of Monolayer Transition Metal Dichalcogenides. Advanced Science, 2021, 8, e2003832.	5.6	25
57	Poor Stability of Li ₂ CO ₃ in the Solid Electrolyte Interphase of a Lithiumâ€Metal Anode Revealed by Cryoâ€Electron Microscopy. Advanced Materials, 2021, 33, e2100404.	11.1	147
58	Self-Perpetuating Carbon Foam Microwave Plasma Conversion of Hydrocarbon Wastes into Useful Fuels and Chemicals. Environmental Science & Technology, 2021, 55, 6239-6247.	4.6	34
59	Switching of metal–oxygen hybridization for selective CO2 electrohydrogenation under mild temperature and pressure. Nature Catalysis, 2021, 4, 274-283.	16.1	77
60	Machine learning for deep elastic strain engineering of semiconductor electronic band structure and effective mass. Npj Computational Materials, 2021, 7, .	3.5	17
61	Tension–compression asymmetry in amorphous silicon. Nature Materials, 2021, 20, 1371-1377.	13.3	36
62	Determining the Criticality of Liâ€Excess for Disorderedâ€Rocksalt Liâ€Ion Battery Cathodes. Advanced Energy Materials, 2021, 11, 2100204.	10.2	31
63	Modeling LiF and FLiBe Molten Salts with Robust Neural Network Interatomic Potential. ACS Applied Materials & Interfaces, 2021, 13, 24582-24592.	4.0	22
64	Airâ€Stable Li <i>_x</i> Al Foil as Freeâ€Standing Electrode with Improved Electrochemical Ductility by Shotâ€Peening Treatment. Advanced Functional Materials, 2021, 31, 2100978.	7.8	17
65	Light-induced static magnetization: Nonlinear Edelstein effect. Physical Review B, 2021, 103, .	1.1	11
66	Dense Allâ€Electrochemâ€Active Electrodes for Allâ€Solidâ€State Lithium Batteries. Advanced Materials, 2021, 33, e2008723.	11.1	26
67	Thermally Aged Li–Mn–O Cathode with Stabilized Hybrid Cation and Anion Redox. Nano Letters, 2021, 21, 4176-4184.	4.5	6
68	Ultralow contact resistance between semimetal and monolayer semiconductors. Nature, 2021, 593, 211-217.	13.7	579
69	Highly efficient parallel grand canonical simulations of interstitial-driven diffusion-deformation processes. Modelling and Simulation in Materials Science and Engineering, 2021, 29, 055018.	0.8	0
70	Hollow-grained "Voronoi foam―ceramics with high strength and thermal superinsulation up to 1400†°C. Materials Today, 2021, 46, 35-43.	8.3	14
71	Topological Phase Transition: Terahertz Driven Reversible Topological Phase Transition of Monolayer Transition Metal Dichalcogenides (Adv. Sci. 12/2021). Advanced Science, 2021, 8, 2170072.	5.6	0
72	Assessing the filtration efficiency and regulatory status of N95s and nontraditional filtering face-piece respirators available during the COVID-19 pandemic. BMC Infectious Diseases, 2021, 21, 712.	1.3	16

#	Article	IF	CITATIONS
73	Lightâ€Induced Quantum Anomalous Hall Effect on the 2D Surfaces of 3D Topological Insulators. Advanced Science, 2021, 8, e2101508.	5.6	11
74	Ultralow Resistance Two‣tage Electrostatically Assisted Air Filtration by Polydopamine Coated PET Coarse Filter. Small, 2021, 17, e2102051.	5.2	40
75	Extreme mixing in nanoscale transition metal alloys. Matter, 2021, 4, 2340-2353.	5.0	102
76	Composition manipulation of bis(fluorosulfonyl)imide-based ionic liquid electrolyte for high-voltage graphite//LiNi0.5Mn1.5O4 lithium-ion batteries. Chemical Engineering Journal, 2021, 415, 128904.	6.6	21
77	CMOS-Compatible Protonic Programmable Resistor Based on Phosphosilicate Glass Electrolyte for Analog Deep Learning. Nano Letters, 2021, 21, 6111-6116.	4.5	25
78	Supercritical CO ₂ â€Assisted SiO <i>_x</i> /Carbon Multiâ€Layer Coating on Si Anode for Lithiumâ€Ion Batteries. Advanced Functional Materials, 2021, 31, 2104135.	7.8	59
79	Pure spin photocurrent in non-centrosymmetric crystals: bulk spin photovoltaic effect. Nature Communications, 2021, 12, 4330.	5.8	51
80	Uranium In Situ Electrolytic Deposition with a Reusable Functional Grapheneâ€Foam Electrode. Advanced Materials, 2021, 33, e2102633.	11.1	52
81	Reusable Polyacrylonitrileâ€Sulfur Extractor of Heavy Metal Ions from Wastewater. Advanced Functional Materials, 2021, 31, 2105845.	7.8	20
82	3D-Printing Damage-Tolerant Architected Metallic Materials with Shape Recoverability via Special Deformation Design of Constituent Material. ACS Applied Materials & Interfaces, 2021, 13, 39915-39924.	4.0	17
83	Designing artificial two-dimensional landscapes via atomic-layer substitution. Proceedings of the National Academy of Sciences of the United States of America, 2021, 118, .	3.3	43
84	Ultralow Resistance Two‣tage Electrostatically Assisted Air Filtration by Polydopamine Coated PET Coarse Filter (Small 33/2021). Small, 2021, 17, 2170172.	5.2	1
85	Peristalsis-like migration of carbon-metabolizing catalytic nanoparticles. Extreme Mechanics Letters, 2021, 49, 101463.	2.0	1
86	A new approach of using Lorentz force to study single-asperity friction inside TEM. Journal of Materials Science and Technology, 2021, 84, 43-48.	5.6	5
87	Towards pressureless sintering of nanocrystalline tungsten. Acta Materialia, 2021, 220, 117344.	3.8	18
88	Electrochemically Engineered, Highly Energy-Efficient Conversion of Ethane to Ethylene and Hydrogen below 550 °C in a Protonic Ceramic Electrochemical Cell. ACS Catalysis, 2021, 11, 12194-12202.	5.5	17
89	De Novo Powered Air-Purifying Respirator Design and Fabrication for Pandemic Response. Frontiers in Bioengineering and Biotechnology, 2021, 9, 690905.	2.0	3
90	Atomic-scale investigation of Lithiation/Delithiation mechanism in High-entropy spinel oxide with superior electrochemical performance. Chemical Engineering Journal, 2021, 420, 129838.	6.6	53

#	Article	IF	CITATIONS
91	Beating 1 Sievert: Optimal Radiation Shielding of Astronauts on a Mission to Mars. Space Weather, 2021, 19, e2021SW002749.	1.3	20
92	Friction and Adhesion Govern Yielding of Disordered Nanoparticle Packings: A Multiscale Adhesive Discrete Element Method Study. Nano Letters, 2021, 21, 7989-7997.	4.5	0
93	High-voltage lithium-metal battery with three-dimensional mesoporous carbon anode host and ether/carbonate binary electrolyte. Carbon, 2021, 184, 752-763.	5.4	10
94	Lithium Plating Mechanism, Detection, and Mitigation in Lithium-Ion Batteries. Progress in Energy and Combustion Science, 2021, 87, 100953.	15.8	117
95	Electrospinning Techniques: Electrospinningâ€Based Strategies for Battery Materials (Adv. Energy) Tj ETQq1 1 0.	.784314 rg 10.2	gBT /Overlock
96	Efficient polysulfide trapping in lithium–sulfur batteries using ultrathin and flexible BaTiO ₃ /graphene oxide/carbon nanotube layers. Nanoscale, 2021, 13, 6863-6870.	2.8	3
97	A Robust Flow-Through Platform for Organic Contaminant Removal. Cell Reports Physical Science, 2021, 2, 100296.	2.8	8
98	Stabilizing electrode–electrolyte interfaces to realize high-voltage Li LiCoO ₂ batteries by a sulfonamide-based electrolyte. Energy and Environmental Science, 2021, 14, 6030-6040.	15.6	84
99	Revealing the BrÃ,nsted-Evans-Polanyi relation in halide-activated fast MoS ₂ growth toward millimeter-sized 2D crystals. Science Advances, 2021, 7, eabj3274.	4.7	18
100	Stable two-dimensional lead iodide hybrid materials for light detection and broadband photoluminescence. Materials Chemistry Frontiers, 2021, 6, 71-77.	3.2	1
101	Sliding ferroelectricity in 2D van der Waals materials: Related physics and future opportunities. Proceedings of the National Academy of Sciences of the United States of America, 2021, 118, .	3.3	83
102	Reusable Polyacrylonitrile‧ulfur Extractor of Heavy Metal Ions from Wastewater (Adv. Funct. Mater.) Tj ETQq0	0 0 rgBT / 7.8	Oyerlock 10
103	First-principles investigation of monatomic gold wires under tension. Computational Materials Science, 2020, 171, 109226.	1.4	4
104	A low-cost intermediate temperature Fe/Graphite battery for grid-scale energy storage. Energy Storage Materials, 2020, 25, 801-810.	9.5	10
105	Optimal annealing of Al foil anode for prelithiation and full-cell cycling in Li-ion battery: The role of grain boundaries in lithiation/delithiation ductility. Nano Energy, 2020, 67, 104274.	8.2	36
106	Focused-helium-ion-beam blow forming of nanostructures: radiation damage and nanofabrication. Nanotechnology, 2020, 31, 045302.	1.3	16
107	Pressureless two-step sintering of ultrafine-grained tungsten. Acta Materialia, 2020, 186, 116-123.	3.8	48
108	FSI-inspired solvent and "full fluorosulfonyl―electrolyte for 4 V class lithium-metal batteries. Energy and Environmental Science, 2020, 13, 212-220.	15.6	198

#	Article	IF	CITATIONS
109	Nanocrystalline Li–Al–Mn–Si Foil as Reversible Li Host: Electronic Percolation and Electrochemical Cycling Stability. Nano Letters, 2020, 20, 896-904.	4.5	33
110	Lithium metal electrode protected by stiff and tough self-compacting separator. Nano Energy, 2020, 69, 104399.	8.2	25
111	Unveiling Nickel Chemistry in Stabilizing Highâ€Voltage Cobaltâ€Rich Cathodes for Lithiumâ€Ion Batteries. Advanced Functional Materials, 2020, 30, 1907903.	7.8	107
112	Is graphite lithiophobic or lithiophilic?. National Science Review, 2020, 7, 1208-1217.	4.6	126
113	Creep-Enabled 3D Solid-State Lithium-Metal Battery. CheM, 2020, 6, 2878-2892.	5.8	63
114	Metallization of diamond. Proceedings of the National Academy of Sciences of the United States of America, 2020, 117, 24634-24639.	3.3	29
115	Superconducting Cu/Nb nanolaminate by coded accumulative roll bonding and its helium damage characteristics. Acta Materialia, 2020, 197, 212-223.	3.8	41
116	Giant Photonic Response of Mexican-Hat Topological Semiconductors for Mid-infrared to Terahertz Applications. Journal of Physical Chemistry Letters, 2020, 11, 6119-6126.	2.1	18
117	Kinetic Rejuvenation of Li-Rich Li-Ion Battery Cathodes upon Oxygen Redox. ACS Applied Energy Materials, 2020, 3, 7931-7943.	2.5	12
118	Ultrastrong adhesion of fluorinated graphene on a substrate: In situ electrochemical conversion to ionic-covalent bonding at the interface. Carbon, 2020, 169, 248-257.	5.4	12
119	Stabilized Coâ€Free Liâ€Rich Oxide Cathode Particles with An Artificial Surface Prereconstruction. Advanced Energy Materials, 2020, 10, 2001120.	10.2	74
120	Hydrogen-Enhanced Vacancy Diffusion in Metals. Journal of Physical Chemistry Letters, 2020, 11, 7015-7020.	2.1	26
121	Periodic Wrinkleâ€Patterned Singleâ€Crystalline Ferroelectric Oxide Membranes with Enhanced Piezoelectricity. Advanced Materials, 2020, 32, e2004477.	11.1	47
122	Metal–Organic Framework–Polyacrylonitrile Composite Beads for Xenon Capture. ACS Applied Materials & Interfaces, 2020, 12, 45342-45350.	4.0	25
123	Sample spinning to mitigate polarization artifact and interstitial-vacancy imbalance in ion-beam irradiation. Npj Computational Materials, 2020, 6, .	3.5	7
124	Coexistence of multi-deformation modes in beta Ti alloys with improved yielding strength and ductility. MATEC Web of Conferences, 2020, 321, 11069.	0.1	0
125	<i>InÂSitu</i> Scanning Transmission Electron Microscopy Observations of Fracture at the Atomic Scale. Physical Review Letters, 2020, 125, 246102.	2.9	34
126	EELS Evidence for Nascent Polymerization of Carbon and Silicon in Amorphization of SiC. Microscopy and Microanalysis, 2020, 26, 648-651.	0.2	0

#	Article	IF	CITATIONS
127	A Surface Se‣ubstituted LiCo[O _{2â^'} <i>_δ</i> Se <i>_δ</i>] Cathode with Ultrastable Highâ€Voltage Cycling in Pouch Fullâ€Cells. Advanced Materials, 2020, 32, e2005182.	11.1	110
128	Sacrificial Poly(propylene carbonate) Membrane for Dispersing Nanoparticles and Preparing Artificial Solid Electrolyte Interphase on Li Metal Anode. ACS Applied Materials & Interfaces, 2020, 12, 27087-27094.	4.0	8
129	Gradient-morph LiCoO ₂ single crystals with stabilized energy density above 3400 W h L ^{â^'1} . Energy and Environmental Science, 2020, 13, 1865-1878.	15.6	118
130	Assessment of the Qualitative Fit Test and Quantitative Single-Pass Filtration Efficiency of Disposable N95 Masks Following Gamma Irradiation. JAMA Network Open, 2020, 3, e209961.	2.8	25
131	Molar-volume asymmetry enabled low-frequency mechanical energy harvesting in electrochemical cells. Applied Energy, 2020, 273, 115230.	5.1	12
132	Radiation-resistant metal-organic framework enables efficient separation of krypton fission gas from spent nuclear fuel. Nature Communications, 2020, 11, 3103.	5.8	54
133	Electrostatic Air Filtration by Multifunctional Dielectric Heterocaking Filters with Ultralow Pressure Drop. ACS Applied Materials & Interfaces, 2020, 12, 29383-29392.	4.0	14
134	Origin of micrometer-scale dislocation motion during hydrogen desorption. Science Advances, 2020, 6, eaaz1187.	4.7	29
135	Manipulation of Nitrogen-Heteroatom Configuration for Enhanced Charge-Storage Performance and Reliability of Nanoporous Carbon Electrodes. ACS Applied Materials & Interfaces, 2020, 12, 32797-32805.	4.0	32
136	Protonic solid-state electrochemical synapse for physical neural networks. Nature Communications, 2020, 11, 3134.	5.8	82
137	Semiâ€Flooded Sulfur Cathode with Ultralean Absorbed Electrolyte in Li–S Battery. Advanced Science, 2020, 7, 1903168.	5.6	40
138	Toward a Safer Battery Management System: A Critical Review on Diagnosis and Prognosis of Battery Short Circuit. IScience, 2020, 23, 101010.	1.9	122
139	Dendrimer-Au Nanoparticle Network Covered Alumina Membrane for Ion Rectification and Enhanced Bioanalysis. Nano Letters, 2020, 20, 1846-1854.	4.5	71
140	Deformation mechanism maps for sub-micron sized aluminum. Acta Materialia, 2020, 188, 570-578.	3.8	11
141	Raftingâ€Enabled Recovery Avoids Recrystallization in 3Dâ€Printingâ€Repaired Singleâ€Crystal Superalloys. Advanced Materials, 2020, 32, e1907164.	11.1	28
142	Normal-to-topological insulator martensitic phase transition in group-IV monochalcogenides driven by light. NPG Asia Materials, 2020, 12, .	3.8	18
143	Molecular Dynamics. , 2020, , 573-594.		6
144	A Novel Moistureâ€Insensitive and Lowâ€Corrosivity Ionic Liquid Electrolyte for Rechargeable Aluminum Batteries. Advanced Functional Materials, 2020, 30, 1909565.	7.8	38

#	Article	IF	CITATIONS
145	Hierarchical {332}<113> twinning in a metastable β Ti-alloy showing tolerance to strain localization. Materials Research Letters, 2020, 8, 247-253.	4.1	35
146	Achieving 5.9% elastic strain in kilograms of metallic glasses: Nanoscopic strain engineering goes macro. Materials Today, 2020, 37, 18-26.	8.3	25
147	Observation of strong higher-order lattice anharmonicity in Raman and infrared spectra. Physical Review B, 2020, 101, .	1.1	43
148	Surpassing lithium metal rechargeable batteries with self-supporting Li–Sn–Sb foil anode. Nano Energy, 2020, 74, 104815.	8.2	28
149	More Efficient and Accurate Simulations of Primary Radiation Damage in Materials with Nanosized Microstructural Features orÂlonÂBeams. , 2020, , 2381-2412.		2
150	Li metal deposition and stripping in a solid-state battery via Coble creep. Nature, 2020, 578, 251-255.	13.7	333
151	Understanding the Interplay between Li Intercalation and Li Plating Using Single Graphite Particle Electrochemistry. ECS Meeting Abstracts, 2020, MA2020-01, 447-447.	0.0	0
152	(Invited) Controlling the Size and Dispersion of Exsolved Catalyst Particles By Electrochemistry and By Strain. ECS Meeting Abstracts, 2020, MA2020-01, 1473-1473.	0.0	0
153	Flexible Ferroelectrics: Periodic Wrinkleâ€Patterned Singleâ€Crystalline Ferroelectric Oxide Membranes with Enhanced Piezoelectricity (Adv. Mater. 50/2020). Advanced Materials, 2020, 32, 2070377.	11.1	0
154	Advanced Electron Microscopy Characterization of Intergranular Corrosion in Ni-20Cr Alloy Under Molten Salt Environment. Microscopy and Microanalysis, 2020, 26, 180-182.	0.2	0
155	Complex Structure of Molten NaCl-CrClx Salts: Octahedra Network and Intermediate-Range Order. ECS Meeting Abstracts, 2020, MA2020-02, 2918-2918.	0.0	0
156	Optomechanical control of stacking patterns of h-BN bilayer. Nano Research, 2019, 12, 2634-2639.	5.8	20
157	Anisotropic mechanical properties and strengthening mechanism in superaligned carbon nanotubes-reinforced aluminum. Carbon, 2019, 153, 513-524.	5.4	12
158	Large plasticity in magnesium mediated by pyramidal dislocations. Science, 2019, 365, 73-75.	6.0	264
159	Near-infrared optical properties and proposed phase-change usefulness of transition metal disulfides. Applied Physics Letters, 2019, 115, .	1.5	19
160	Electron-Beam Manipulation of Lattice Impurities in Graphene and Single-Walled Carbon Nanotubes. Microscopy and Microanalysis, 2019, 25, 938-939.	0.2	0
161	Snâ€Alloy Foil Electrode with Mechanical Prelithiation: Fullâ€Cell Performance up to 200 Cycles. Advanced Energy Materials, 2019, 9, 1902150.	10.2	37
162	Batteries: Snâ€Alloy Foil Electrode with Mechanical Prelithiation: Fullâ€Cell Performance up to 200 Cycles (Adv. Energy Mater. 42/2019). Advanced Energy Materials, 2019, 9, 1970165.	10.2	1

ARTICLE IF CITATIONS Dynamic Fluidâ€Like Graphene with Ultralow Frictional Molecular Bearing. Advanced Materials, 2019, 31, 11.1 e1903195. Super-elastic ferroelectric single-crystal membrane with continuous electric dipole rotation. 164 6.0 272 Science, 2019, 366, 475-479. Manipulating Sulfur Mobility Enables Advanced Li-S Batteries. Matter, 2019, 1, 1047-1060. 5.0 In-Situ Observation of Concurrent Oxidation and Mechanical Deformation in Al and Zr. Microscopy 166 0.2 0 and Microanalysis, 2019, 25, 1912-1913. Designing solid solution hardening to retain uniform ductility while quadrupling yield strength. 3.8 Acta Materialia, 2019, 179, 107-118. Waterproof molecular monolayers stabilize 2D materials. Proceedings of the National Academy of 168 3.3 32 Sciences of the United States of America, 2019, 116, 20844-20849. Controlled growth of single-crystalline metal nanowires via thermomigration across a nanoscale 5.8 16 junction. Nature Communications, 2019, 10, 4478. Making metals linear super-elastic with ultralow modulus and nearly zero hysteresis. Materials 170 6.4 27 Horizons, 2019, 6, 515-523. More Efficient and Accurate Simulations of Primary Radiation Damage in Materials with Nanosized Microstructural Features or Ion Beams. , 2019, , 1-33. 171 The role of chemical disorder and structural freedom in radiation-induced amorphization of silicon 172 carbide deduced from electron spectroscopy and ab initio simulations. Journal of Nuclear Materials, 1.3 9 2019, 514, 299-310. Hybrid electrolyte enables safe and practical 5 V LiNi_{0.5}Mn_{1.5}O₄ bátteries. Journal of Materials Chemistry A, 2019, 7, 16516-16525. Gassing in Sn-Anode Sodium-Ion Batteries and Its Remedy by Metallurgically Prealloying Na. ACS Applied 174 4.0 37 Materials & amp; Interfaces, 2019, 11, 23207-23212. Roll-to-roll prelithiation of Sn foil anode suppresses gassing and enables stable full-cell cycling of 15.6 147 lithium ion batteries. Energy and Environmental Science, 2019, 12, 2991-3000. Engineering single-atom dynamics with electron irradiation. Science Advances, 2019, 5, eaav2252. 176 4.7 61 Colloidal quasi-one-dimensional dual semiconductor core/shell nanorod couple heterostructures 2.8 with blue fluorescence. Nanoscale, 2019, 11, 10190-10197. Niobium oxide dihalides NbOX₂: a new family of two-dimensional van der Waals layered materials with intrinsic ferroelectricity and antiferroelectricity. Nanoscale Horizons, 2019, 4, 178 4.1 43 1113-1123. Two-Dimensional Silver(I)-Dithiocarboxylate Coordination Polymer Exhibiting Strong Near-Infrared 179 28 Photothermal Effect. Inorganic Chemistry, 2019, 58, 6601-6608.

Ju Li

180Low-temperature synthesized Li₄Mn₅O₁₂-like cathode with hybrid
cation- and anion-redox capacities. Chemical Communications, 2019, 55, 8118-8121.2.221

#	Article	IF	CITATIONS
181	Intercalation-conversion hybrid cathodes enabling Li–S full-cell architectures with jointly superior gravimetric and volumetric energy densities. Nature Energy, 2019, 4, 374-382.	19.8	449
182	Strong and ductile beta Ti–18Zr–13Mo alloy with multimodal twinning. Materials Research Letters, 2019, 7, 251-257.	4.1	69
183	Microwave growth and tunable photoluminescence of nitrogen-doped graphene and carbon nitride quantum dots. Journal of Materials Chemistry C, 2019, 7, 5468-5476.	2.7	75
184	Slip transmission assisted by Shockley partials across <mml:math xmlns:mml="http://www.w3.org/1998/Math/MathML" altimg="si1.gif" overflow="scroll"><mml:mrow><mml:mi>l±</mml:mi><mml:mo>/</mml:mo><mml:mi>l²</mml:mi></mml:mrow> interfaces in Ti-alloys. Acta Materialia, 2019, 171, 291-305.</mml:math 	>< ∄ ħml:ma	ith7
185	Full-Cell Cycling of a Self-Supporting Aluminum Foil Anode with a Phosphate Conversion Coating. ACS Applied Materials & Interfaces, 2019, 11, 15656-15661.	4.0	27
186	Mechanism of hardening and damage initiation in oxygen embrittlement of body-centred-cubic niobium. Acta Materialia, 2019, 168, 331-342.	3.8	60
187	Deep elastic strain engineering of bandgap through machine learning. Proceedings of the National Academy of Sciences of the United States of America, 2019, 116, 4117-4122.	3.3	70
188	Additive manufacturing of patterned 2D semiconductor through recyclable masked growth. Proceedings of the National Academy of Sciences of the United States of America, 2019, 116, 3437-3442.	3.3	46
189	An ethyl methyl sulfone co-solvent eliminates macroscopic morphological instabilities of lithium metal anode. Chemical Communications, 2019, 55, 3387-3389.	2.2	8
190	High-performance sodium-ion batteries with a hard carbon anode: transition from the half-cell to full-cell perspective. Nanoscale, 2019, 11, 22196-22205.	2.8	75
191	Gradient Li-rich oxide cathode particles immunized against oxygen release by a molten salt treatment. Nature Energy, 2019, 4, 1049-1058.	19.8	248
192	Stronger role of four-phonon scattering than three-phonon scattering in thermal conductivity of III-V semiconductors at room temperature. Physical Review B, 2019, 100, .	1.1	72
193	Superior electrochemical performance of sodium-ion full-cell using poplar wood derived hard carbon anode. Energy Storage Materials, 2019, 18, 269-279.	9.5	94
194	Graphene-coated tungsten nanowires deliver unprecedented modulus and strength. Materials Research Letters, 2019, 7, 47-52.	4.1	9
195	Brownian-snowball-mechanism-induced hierarchical cobalt sulfide for supercapacitors. Journal of Power Sources, 2019, 412, 321-330.	4.0	31
196	Moderately concentrated electrolyte improves solid–electrolyte interphase and sodium storage performance of hard carbon. Energy Storage Materials, 2019, 16, 146-154.	9.5	73
197	Liquid-Like, Self-Healing Aluminum Oxide during Deformation at Room Temperature. Nano Letters, 2018, 18, 2492-2497.	4.5	91
198	Intragranular Dispersion of Carbon Nanotubes Comprehensively Improves Aluminum Alloys. Advanced Science, 2018, 5, 1800115.	5.6	20

#	Article	IF	CITATIONS
199	Carbon nanotubes and manganese oxide hybrid nanostructures as high performance fiber supercapacitors. Communications Chemistry, 2018, 1, .	2.0	32
200	Capacity extended bismuth-antimony cathode for high-performance liquid metal battery. Journal of Power Sources, 2018, 381, 38-45.	4.0	43
201	Insight from in situ microscopy into which precipitate morphology can enable high strength in magnesium alloys. Journal of Materials Science and Technology, 2018, 34, 1061-1066.	5.6	60
202	Fluorine-donating electrolytes enable highly reversible 5-V-class Li metal batteries. Proceedings of the National Academy of Sciences of the United States of America, 2018, 115, 1156-1161.	3.3	512
203	Low-Temperature Copper Bonding Strategy with Graphene Interlayer. ACS Nano, 2018, 12, 2395-2402.	7.3	49
204	SnSeÂ+ÂAg2Se composite engineering with ball milling for enhanced thermoelectric performance. Rare Metals, 2018, 37, 333-342.	3.6	24
205	Nano-beam and nano-target effects in ion radiation. Nanoscale, 2018, 10, 1598-1606.	2.8	14
206	Three-dimensional carbon framework anode improves sodiation–desodiation properties in ionic liquid electrolyte. Nano Energy, 2018, 49, 515-522.	8.2	20
207	Carbothermal shock synthesis of high-entropy-alloy nanoparticles. Science, 2018, 359, 1489-1494.	6.0	1,065
208	Functional Group-Dependent Supercapacitive and Aging Properties of Activated Carbon Electrodes in Organic Electrolyte. ACS Sustainable Chemistry and Engineering, 2018, 6, 1208-1214.	3.2	41
209	Sample-size-dependent surface dislocation nucleation in nanoscale crystals. Acta Materialia, 2018, 145, 19-29.	3.8	52
210	Ultrastretchable carbon nanotube composite electrodes for flexible lithium-ion batteries. Nanoscale, 2018, 10, 19972-19978.	2.8	46
211	Opto-Mechanics Driven Fast Martensitic Transition in Two-Dimensional Materials. Nano Letters, 2018, 18, 7794-7800.	4.5	38
212	Electrochemically-mediated selective capture of heavy metal chromium and arsenic oxyanions from water. Nature Communications, 2018, 9, 4701.	5.8	193
213	Origin of Two-Dimensional Vertical Ferroelectricity in WTe ₂ Bilayer and Multilayer. Journal of Physical Chemistry Letters, 2018, 9, 7160-7164.	2.1	168
214	TiO ₂ -Nanocoated Black Phosphorus Electrodes with Improved Electrochemical Performance. ACS Applied Materials & Interfaces, 2018, 10, 36058-36066.	4.0	23
215	Interactions between Lithium Growths and Nanoporous Ceramic Separators. Joule, 2018, 2, 2434-2449.	11.7	180
216	Turning a native or corroded Mg alloy surface into an anti-corrosion coating in excited CO2. Nature Communications, 2018, 9, 4058.	5.8	76

#	Article	IF	CITATIONS
217	A Waterâ€Soluble NaCMC/NaPAA Binder for Exceptional Improvement of Sodiumâ€Ion Batteries with an SnO ₂ â€Ordered Mesoporous Carbon Anode. ChemSusChem, 2018, 11, 3923-3931.	3.6	34
218	Monte Carlo simulation of PKA distribution along nanowires under ion radiation. Nuclear Engineering and Design, 2018, 340, 300-307.	0.8	7
219	Atomically sharp interlayer stacking shifts at anti-phase grain boundaries in overlapping MoS ₂ secondary layers. Nanoscale, 2018, 10, 16692-16702.	2.8	22
220	Caution Is Needed in Operating and Managing the Waste of New Pebble-Bed Nuclear Reactors. Joule, 2018, 2, 1911-1914.	11.7	10
221	Fluorophosphates from Solid‣tate Synthesis and Electrochemical Ion Exchange: NaVPO ₄ F or Na ₃ V ₂ (PÓ ₄) ₂ F ₃ ?. Advanced Energy Materials, 2018, 8, 1801064.	10.2	57
222	MnO2 nanoparticles anchored on carbon nanotubes with hybrid supercapacitor-battery behavior for ultrafast lithium storage. Carbon, 2018, 139, 145-155.	5.4	77
223	Ultrathin HfO2-modified carbon nanotube films as efficient polysulfide barriers for Li-S batteries. Carbon, 2018, 139, 896-905.	5.4	33
224	Bimetallic Nanoparticle Oxidation in Three Dimensions by Chemically Sensitive Electron Tomography and <i>in Situ</i> Transmission Electron Microscopy. ACS Nano, 2018, 12, 7866-7874.	7.3	49
225	Reduced expansion and improved full-cell cycling of a SnO _x #C embedded structure for lithium-ion batteries. Journal of Materials Chemistry A, 2018, 6, 15738-15746.	5.2	9
226	Colloidal synthesis of 1T' phase dominated WS2 towards endurable electrocatalysis. Nano Energy, 2018, 50, 176-181.	8.2	123
227	Developing Highâ€Performance Lithium Metal Anode in Liquid Electrolytes: Challenges and Progress. Advanced Materials, 2018, 30, e1706375.	11.1	335
228	A soft non-porous separator and its effectiveness in stabilizing Li metal anodes cycling at 10 mA cm ^{â^2} observed in situ in a capillary cell. Journal of Materials Chemistry A, 2017, 5, 4300-4307.	5.2	66
229	Self-healing SEI enables full-cell cycling of a silicon-majority anode with a coulombic efficiency exceeding 99.9%. Energy and Environmental Science, 2017, 10, 580-592.	15.6	421
230	A computational study of yttria-stabilized zirconia: II. Cation diffusion. Acta Materialia, 2017, 126, 438-450.	3.8	52
231	A computational study of yttria-stabilized zirconia: I. Using crystal chemistry to search for the ground state on a glassy energy landscape. Acta Materialia, 2017, 127, 73-84.	3.8	25
232	Non-conservative dynamics of lattice sites near a migrating interface in a diffusional phase transformation. Acta Materialia, 2017, 127, 481-490.	3.8	9
233	Effect of hydrogen on the integrity of aluminium–oxide interface at elevated temperatures. Nature Communications, 2017, 8, 14564.	5.8	39
234	Coordination Polymers Derived General Synthesis of Multishelled Mixed Metalâ€Oxide Particles for Hybrid Supercapacitors. Advanced Materials, 2017, 29, 1605902.	11.1	345

#	Article	IF	CITATIONS
235	High temperature ferromagnetism in π-conjugated two-dimensional metal–organic frameworks. Chemical Science, 2017, 8, 2859-2867.	3.7	86
236	Helium Nanobubbles Enhance Superelasticity and Retard Shear Localization in Small-Volume Shape Memory Alloy. Nano Letters, 2017, 17, 3725-3730.	4.5	24
237	Low-Temperature Carbon Coating of Nanosized Li _{1.015} Al _{0.06} Mn _{1.925} O ₄ and High-Density Electrode for High-Power Li-Ion Batteries. Nano Letters, 2017, 17, 3744-3751.	4.5	45
238	Electrochemomechanical degradation of high-capacity battery electrode materials. Progress in Materials Science, 2017, 89, 479-521.	16.0	144
239	Conductive graphene oxide-polyacrylic acid (GOPAA) binder for lithium-sulfur battery. Nano Energy, 2017, 31, 568-574.	8.2	147
240	Mechanics of electrochemically driven mechanical energy harvesting. Extreme Mechanics Letters, 2017, 15, 78-82.	2.0	5
241	Double-oxide sulfur host for advanced lithium-sulfur batteries. Nano Energy, 2017, 38, 12-18.	8.2	93
242	Influence of nanoscale structural heterogeneity on shear banding in metallic glasses. Acta Materialia, 2017, 134, 104-115.	3.8	42
243	Ion radiation albedo effect: influence of surface roughness on ion implantation and sputtering of materials. Nuclear Fusion, 2017, 57, 016038.	1.6	25
244	Small-volume aluminum alloys with native oxide shell deliver unprecedented strength and toughness. Acta Materialia, 2017, 126, 202-209.	3.8	28
245	Ti3+-free three-phase Li4Ti5O12/TiO2 for high-rate lithium ion batteries: Capacity and conductivity enhancement by phase boundaries. Nano Energy, 2017, 32, 294-301.	8.2	110
246	Liquid cell transmission electron microscopy observation of lithium metal growth and dissolution: Root growth, dead lithium and lithium flotsams. Nano Energy, 2017, 32, 271-279.	8.2	361
247	Sliding of coherent twin boundaries. Nature Communications, 2017, 8, 1108.	5.8	44
248	Organic Thiocarboxylate Electrodes for a Roomâ€īemperature Sodiumâ€ion Battery Delivering an Ultrahigh Capacity. Angewandte Chemie - International Edition, 2017, 56, 15334-15338.	7.2	91
249	Gravimetric and volumetric energy densities of lithium-sulfur batteries. Current Opinion in Electrochemistry, 2017, 6, 92-99.	2.5	100
250	Revealing the Bonding of Nitrogen Impurities in Monolayer Graphene. Microscopy and Microanalysis, 2017, 23, 1750-1751.	0.2	1
251	Lithium titanate hydrates with superfast and stable cycling in lithium ion batteries. Nature Communications, 2017, 8, 627.	5.8	110
252	Hydrothermal synthesis of SnQ (<i>Q</i> = Te, Se, S) and their thermoelectric properties. Nanotechnology, 2017, 28, 455707.	1.3	24

#	Article	IF	CITATIONS
253	Signature of Metallic Behavior in the Metal–Organic Frameworks M ₃ (hexaiminobenzene) ₂ (M = Ni, Cu). Journal of the American Chemical Society, 2017, 139, 13608-13611.	6.6	324
254	<i>Ad hoc</i> solid electrolyte on acidized carbon nanotube paper improves cycle life of lithium–sulfur batteries. Energy and Environmental Science, 2017, 10, 2544-2551.	15.6	82
255	A high-performance sodium-ion battery enhanced by macadamia shell derived hard carbon anode. Nano Energy, 2017, 39, 489-498.	8.2	172
256	Nitrogen-Doped Carbon for Sodium-Ion Battery Anode by Self-Etching and Graphitization of Bimetallic MOF-Based Composite. CheM, 2017, 3, 152-163.	5.8	228
257	A thin multifunctional coating on a separator improves the cyclability and safety of lithium sulfur batteries. Chemical Science, 2017, 8, 6619-6625.	3.7	94
258	Structure-property relationships from universal signatures of plasticity in disordered solids. Science, 2017, 358, 1033-1037.	6.0	218
259	How Solid-Electrolyte Interphase Forms in Aqueous Electrolytes. Journal of the American Chemical Society, 2017, 139, 18670-18680.	6.6	365
260	Effect of nonlinear and noncollinear transformation strain pathways in phase-field modeling of nucleation and growth during martensite transformation. Npj Computational Materials, 2017, 3, .	3.5	13
261	Conetronics in 2D metal-organic frameworks: double/half Dirac cones and quantum anomalous Hall effect. 2D Materials, 2017, 4, 015015.	2.0	41
262	Nanoscratching of copper surface by CeO2. Acta Materialia, 2017, 124, 343-350.	3.8	47
263	Organic Thiocarboxylate Electrodes for a Roomâ€Temperature Sodiumâ€Ion Battery Delivering an Ultrahigh Capacity. Angewandte Chemie, 2017, 129, 15536-15540.	1.6	31
264	Parallel Stitching of 2D Materials. Advanced Materials, 2016, 28, 2322-2329.	11.1	195
265	Crystal metamorphosis at stress extremes: how soft phonons turn into lattice defects. NPG Asia Materials, 2016, 8, e320-e320.	3.8	8
266	Accelerating ferroic ageing dynamics upon cooling. NPG Asia Materials, 2016, 8, e319-e319.	3.8	7
267	Metal-nanotube composites as radiation resistant materials. Applied Physics Letters, 2016, 109, .	1.5	11
268	Ferroelasticity and domain physics in two-dimensional transition metal dichalcogenide monolayers. Nature Communications, 2016, 7, 10843.	5.8	125
269	Ton-scale metal–carbon nanotube composite: The mechanism of strengthening while retaining tensile ductility. Extreme Mechanics Letters, 2016, 8, 245-250.	2.0	30
270	Enhanced electrochemical performance promoted by monolayer graphene and void space in silicon composite anode materials. Nano Energy, 2016, 27, 647-657.	8.2	61

#	Article	IF	CITATIONS
271	Chestnut-like SnO2/C nanocomposites with enhanced lithium ion storage properties. Nano Energy, 2016, 30, 885-891.	8.2	64
272	Topological semimetal to insulator quantum phase transition in the Zintl compounds <mml:math xmlns:mml="http://www.w3.org/1998/Math/MathML"><mml:mrow><mml:mi mathvariant="normal">B<mml:msub><mml:mi mathvariant="normal">a<mml:msub><mml:mi></mml:mi></mml:msub><mml:msub><mml:mi>X</mml:mi>X Physical Review B, 2016, 94, .</mml:msub></mml:mi </mml:msub></mml:mi </mml:mrow></mml:math 	1.1 nl:mo>(</td <td>24 mml:mo><mr< td=""></mr<></td>	24 mml:mo> <mr< td=""></mr<>
273	Strongly correlated breeding of high-speed dislocations. Acta Materialia, 2016, 119, 229-241.	3.8	21
274	Transition of lithium growth mechanisms in liquid electrolytes. Energy and Environmental Science, 2016, 9, 3221-3229.	15.6	1,054
275	Triple Point Topological Metals. Physical Review X, 2016, 6, .	2.8	273
276	In-Plane Optical Anisotropy of Layered Gallium Telluride. ACS Nano, 2016, 10, 8964-8972.	7.3	179
277	The evolving quality of frictional contact with graphene. Nature, 2016, 539, 541-545.	13.7	389
278	Synthesis of Highâ€Quality Largeâ€Area Homogenous 1T′ MoTe ₂ from Chemical Vapor Deposition. Advanced Materials, 2016, 28, 9526-9531.	11.1	125
279	In situ TEM study of deformation-induced crystalline-to-amorphous transition in silicon. NPG Asia Materials, 2016, 8, e291-e291.	3.8	60
280	Surface Rebound of Relativistic Dislocations Directly and Efficiently Initiates Deformation Twinning. Physical Review Letters, 2016, 117, 165501.	2.9	6
281	Nanobubble Fragmentation and Bubble-Free-Channel Shear Localization in Helium-Irradiated Submicron-Sized Copper. Physical Review Letters, 2016, 117, 215501.	2.9	61
282	Approaching the ideal elastic strain limit in silicon nanowires. Science Advances, 2016, 2, e1501382.	4.7	169
283	Hydrogenated vacancies lock dislocations in aluminium. Nature Communications, 2016, 7, 13341.	5.8	131
284	Enhanced thermoelectric properties of SnSe polycrystals via texture control. Physical Chemistry Chemical Physics, 2016, 18, 31821-31827.	1.3	53
285	Room temperature stable CO _{<i>x</i>} -free H ₂ production from methanol with magnesium oxide nanophotocatalysts. Science Advances, 2016, 2, e1501425.	4.7	62
286	Anion-redox nanolithia cathodes for Li-ion batteries. Nature Energy, 2016, 1, .	19.8	171
287	Strain-engineered diffusive atomic switching in two-dimensional crystals. Nature Communications, 2016, 7, 11983.	5.8	85
288	Radiation-Induced Helium Nanobubbles Enhance Ductility in Submicron-Sized Single-Crystalline Copper. Nano Letters, 2016, 16, 4118-4124.	4.5	102

#	Article	IF	CITATIONS
289	Lithium–Boron (Li–B) Monolayers: First-Principles Cluster Expansion and Possible Two-Dimensional Superconductivity. ACS Applied Materials & Interfaces, 2016, 8, 2526-2532.	4.0	49
290	Coupling and Stacking Order of ReS ₂ Atomic Layers Revealed by Ultralow-Frequency Raman Spectroscopy. Nano Letters, 2016, 16, 1404-1409.	4.5	139
291	Dispersion of carbon nanotubes in aluminum improves radiation resistance. Nano Energy, 2016, 22, 319-327.	8.2	55
292	Sample size effects on strength and deformation mechanism of Sc75Fe25 nanoglass and metallic glass. Scripta Materialia, 2016, 116, 95-99.	2.6	69
293	Shuffling-controlled versus strain-controlled deformation twinning: The case for HCP Mg twin nucleation. International Journal of Plasticity, 2016, 82, 32-43.	4.1	71
294	Retaining Large and Adjustable Elastic Strains of Kilogram-Scale Nb Nanowires. ACS Applied Materials & Interfaces, 2016, 8, 2917-2922.	4.0	21
295	Ruddlesden–Popper perovskite sulfides A3B2S7: A new family of ferroelectric photovoltaic materials for the visible spectrum. Nano Energy, 2016, 22, 507-513.	8.2	66
296	Periodic stacking of 2D charged sheets: Self-assembled superlattice of Ni–Al layered double hydroxide (LDH) and reduced graphene oxide. Nano Energy, 2016, 20, 185-193.	8.2	188
297	Ultra-large suspended graphene as a highly elastic membrane for capacitive pressure sensors. Nanoscale, 2016, 8, 3555-3564.	2.8	100
298	Electrochemically driven mechanical energy harvesting. Nature Communications, 2016, 7, 10146.	5.8	123
299	Size-Dependent Brittle-to-Ductile Transition in Silica Glass Nanofibers. Nano Letters, 2016, 16, 105-113.	4.5	120
300	Oxidation of ferritic and ferritic–martensitic steels in flowing and static supercritical water. Corrosion Science, 2016, 103, 124-131.	3.0	78
301	Does p-type ohmic contact exist in WSe ₂ –metal interfaces?. Nanoscale, 2016, 8, 1179-1191.	2.8	166
302	IM3D: A parallel Monte Carlo code for efficient simulations of primary radiation displacements and damage in 3D geometry. Scientific Reports, 2015, 5, 18130.	1.6	43
303	Stress-driven crystallization via shear-diffusion transformations in a metallic glass at very low temperatures. Physical Review B, 2015, 91, .	1.1	25
304	Deformation-driven diffusion and plastic flow in amorphous granular pillars. Physical Review E, 2015, 91, 062212.	0.8	27
305	Proximity-Driven Enhanced Magnetic Order at Ferromagnetic-Insulator–Magnetic-Topological-Insulator Interface. Physical Review Letters, 2015, 115, 087201.	2.9	81
306	Giant piezoelectricity of monolayer group IV monochalcogenides: SnSe, SnS, GeSe, and GeS. Applied Physics Letters, 2015, 107, .	1.5	569

#	Article	IF	CITATIONS
307	Controlled Rejuvenation of Amorphous Metals with Thermal Processing. Scientific Reports, 2015, 5, 10545.	1.6	110
308	Piezoelectricity in two-dimensional group-III monochalcogenides. Nano Research, 2015, 8, 3796-3802.	5.8	219
309	Ultrafast shape change and joining of small-volume materials using nanoscale electrical discharge. Nano Research, 2015, 8, 2143-2151.	5.8	15
310	Effect of twin boundaries and structural polytypes on electron transport in GaAs. Computational Materials Science, 2015, 108, 258-263.	1.4	15
311	Slurryless Li ₂ S/Reduced Graphene Oxide Cathode Paper for High-Performance Lithium Sulfur Battery. Nano Letters, 2015, 15, 1796-1802.	4.5	252
312	Ripplocations in van der Waals Layers. Nano Letters, 2015, 15, 1302-1308.	4.5	114
313	Transitions from Near-Surface to Interior Redox upon Lithiation in Conversion Electrode Materials. Nano Letters, 2015, 15, 1437-1444.	4.5	97
314	Layer-Dependent Modulation of Tungsten Disulfide Photoluminescence by Lateral Electric Fields. ACS Nano, 2015, 9, 2740-2748.	7.3	50
315	Flow Stress in Submicron BCC Iron Single Crystals: Sample-size-dependent Strain-rate Sensitivity and Rate-dependent Size Strengthening. Materials Research Letters, 2015, 3, 121-127.	4.1	28
316	Modelling of stacked 2D materials and devices. 2D Materials, 2015, 2, 032003.	2.0	59
317	The interaction of dislocations and hydrogen-vacancy complexes and its importance for deformation-induced proto nano-voids formation in α-Fe. International Journal of Plasticity, 2015, 74, 175-191.	4.1	144
318	Diffusive origins. Nature Materials, 2015, 14, 656-657.	13.3	28
319	Optoelectronic crystal of artificial atoms in strain-textured molybdenum disulphide. Nature Communications, 2015, 6, 7381.	5.8	331
320	In situ study of the initiation of hydrogen bubbles at the aluminium metal/oxide interface. Nature Materials, 2015, 14, 899-903.	13.3	134
321	Multiple stiffening effects of nanoscale knobs on human red blood cells infected with <i>Plasmodium falciparum</i> malaria parasite. Proceedings of the National Academy of Sciences of the United States of America, 2015, 112, 6068-6073.	3.3	108
322	Experimental Verification of the Van Vleck Nature of Long-Range Ferromagnetic Order in the Vanadium-Doped Three-Dimensional Topological Insulator <mml:math xmlns:mml="http://www.w3.org/1998/Math/MathML" display="inline"><mml:mrow><mml:msub><mml:mrow><mml:mi>Sb</mml:mi></mml:mrow><mml:mrow><mm< td=""><td>2.9 l:mn>2<td>79 nml:mn></td></td></mm<></mml:mrow></mml:msub></mml:mrow></mml:math 	2.9 l:mn>2 <td>79 nml:mn></td>	79 nml:mn>
323	Physical Review Letters, 2015, 114, 146802. From "Smaller is Stronger―to "Sizeâ€Independent Strength Plateau― Towards Measuring the Ideal Strength of Iron. Advanced Materials, 2015, 27, 3385-3390.	11.1	62
324	Directing the Deformation Paths of Soft Metamaterials with Prescribed Asymmetric Units. Advanced Materials, 2015, 27, 2747-2752.	11.1	60

#	Article	IF	CITATIONS
325	Inelastic x-ray scattering measurements of phonon dispersion and lifetimes in PbTe _{1â^'<i>x</i>} Se <i>_x</i> alloys. Journal of Physics Condensed Matter, 2015, 27, 375403.	0.7	14
326	In situ study of the mechanical properties of airborne haze particles. Science China Technological Sciences, 2015, 58, 2046-2051.	2.0	6
327	Growth Conditions Control the Elastic and Electrical Properties of ZnO Nanowires. Nano Letters, 2015, 15, 7886-7892.	4.5	53
328	Charging/Discharging Nanomorphology Asymmetry and Rate-Dependent Capacity Degradation in Li–Oxygen Battery. Nano Letters, 2015, 15, 8260-8265.	4.5	97
329	Cyclic deformation leads to defect healing and strengthening of small-volume metal crystals. Proceedings of the National Academy of Sciences of the United States of America, 2015, 112, 13502-13507.	3.3	40
330	Diffusive versus Displacive Contact Plasticity of Nanoscale Asperities: Temperature- and Velocity-Dependent Strongest Size. Nano Letters, 2015, 15, 6582-6585.	4.5	35
331	Pie-like electrode design for high-energy density lithium–sulfur batteries. Nature Communications, 2015, 6, 8850.	5.8	453
332	Plasticity of a scandium-based nanoglass. Scripta Materialia, 2015, 98, 40-43.	2.6	114
333	Topological crystalline insulator nanomembrane with strain-tunable band gap. Nano Research, 2015, 8, 967-979.	5.8	56
334	Allâ€Metallic Vertical Transistors Based on Stacked Dirac Materials. Advanced Functional Materials, 2015, 25, 68-77.	7.8	59
335	Uniaxial stress-driven coupled grain boundary motion in hexagonal close-packed metals: A molecular dynamics study. Acta Materialia, 2015, 82, 295-303.	3.8	28
336	Envelope function method for electrons in slowly-varying inhomogeneously deformed crystals. Journal of Physics Condensed Matter, 2014, 26, 455801.	0.7	1
337	Engineering the shape and structure of materials by fractal cut. Proceedings of the National Academy of Sciences of the United States of America, 2014, 111, 17390-17395.	3.3	265
338	Theoretical study of the ammonia nitridation rate on an Fe (100) surface: A combined density functional theory and kinetic Monte Carlo study. Journal of Chemical Physics, 2014, 141, 134108.	1.2	3
339	Twinning-like lattice reorientation without a crystallographic twinning plane. Nature Communications, 2014, 5, 3297.	5.8	154
340	Extended defects, ideal strength and actual strengths of finite-sized metallic glasses. Acta Materialia, 2014, 73, 149-166.	3.8	31
341	In Situ Observation of Random Solid Solution Zone in LiFePO ₄ Electrode. Nano Letters, 2014, 14, 4005-4010.	4.5	104
342	Tailoring Exciton Dynamics by Elastic Strainâ€Gradient in Semiconductors. Advanced Materials, 2014, 26, 2572-2579.	11.1	76

#	Article	IF	CITATIONS
343	Elastic strain engineering for unprecedented materials properties. MRS Bulletin, 2014, 39, 108-114.	1.7	214
344	Quantum spin Hall effect in two-dimensional transition metal dichalcogenides. Science, 2014, 346, 1344-1347.	6.0	1,558
345	Direct observation of hierarchical nucleation of martensite and size-dependent superelasticity in shape memory alloys. Nanoscale, 2014, 6, 2067.	2.8	16
346	Unexpected High-Temperature Stability of β-Zn ₄ Sb ₃ Opens the Door to Enhanced Thermoelectric Performance. Journal of the American Chemical Society, 2014, 136, 1497-1504.	6.6	115
347	Scalable synthesis of a sulfur nanosponge cathode for a lithium–sulfur battery with improved cyclability. Journal of Materials Chemistry A, 2014, 2, 19788-19796.	5.2	12
348	Deviatoric Stress-Driven Fusion of Nanoparticle Superlattices. Nano Letters, 2014, 14, 4951-4958.	4.5	37
349	Tunable Exciton Funnel Using Moiré Superlattice in Twisted van der Waals Bilayer. Nano Letters, 2014, 14, 5350-5357.	4.5	55
350	Liquid-like pseudoelasticity of sub-10-nm crystalline silver particles. Nature Materials, 2014, 13, 1007-1012.	13.3	255
351	Direct Observation of Metal–Insulator Transition in Single-Crystalline Germanium Telluride Nanowire Memory Devices Prior to Amorphization. Nano Letters, 2014, 14, 2201-2209.	4.5	59
352	An index for deformation controllability of small-volume materials. Science China Technological Sciences, 2014, 57, 663-670.	2.0	10
353	A nanoporous oxide interlayer makes a better Pt catalyst on a metallic substrate: Nanoflowers on a nanotube bed. Nano Research, 2014, 7, 1007-1017.	5.8	23
354	Collective nature of plasticity in mediating phase transformation under shock compression. Physical Review B, 2014, 89, .	1.1	40
355	Predicting structure and energy of dislocations and grain boundaries. Acta Materialia, 2014, 74, 125-131.	3.8	54
356	Strain-controlled thermal conductivity in ferroic twinned films. Scientific Reports, 2014, 4, 6375.	1.6	39
357	Study of architectural responses of 3D periodic cellular materials. Modelling and Simulation in Materials Science and Engineering, 2013, 21, 065018.	0.8	9
358	Real-time, high-resolution study of nanocrystallization and fatigue cracking in a cyclically strained metallic glass. Proceedings of the National Academy of Sciences of the United States of America, 2013, 110, 19725-19730.	3.3	61
359	Reducing deformation anisotropy to achieve ultrahigh strength and ductility in Mg at the nanoscale. Proceedings of the National Academy of Sciences of the United States of America, 2013, 110, 13289-13293.	3.3	111
360	Probing the Failure Mechanism of SnO ₂ Nanowires for Sodium-Ion Batteries. Nano Letters, 2013, 13, 5203-5211.	4.5	270

#	Article	IF	CITATIONS
361	In Situ Atomicâ€Scale Imaging of Phase Boundary Migration in FePO ₄ Microparticles During Electrochemical Lithiation. Advanced Materials, 2013, 25, 5461-5466.	11.1	119
362	Origin of Size Dependency in Coherent-Twin-Propagation-Mediated Tensile Deformation of Noble Metal Nanowires. Nano Letters, 2013, 13, 5112-5116.	4.5	88
363	A Transforming Metal Nanocomposite with Large Elastic Strain, Low Modulus, and High Strength. Science, 2013, 339, 1191-1194.	6.0	241
364	Heterogeneously randomized STZ model of metallic glasses: Softening and extreme value statistics during deformation. International Journal of Plasticity, 2013, 40, 1-22.	4.1	78
365	Stress generation during lithiation of high-capacity electrode particles in lithium ion batteries. Acta Materialia, 2013, 61, 4354-4364.	3.8	183
366	Nanowire liquid pumps. Nature Nanotechnology, 2013, 8, 277-281.	15.6	96
367	Competition of shape and interaction patchiness for self-assembling nanoplates. Nature Chemistry, 2013, 5, 466-473.	6.6	278
368	Engineering Catalytic Contacts and Thermal Stability: Gold/Iron Oxide Binary Nanocrystal Superlattices for CO Oxidation. Journal of the American Chemical Society, 2013, 135, 1499-1505.	6.6	122
369	Visualizing size-dependent deformation mechanism transition in Sn. Scientific Reports, 2013, 3, 2113.	1.6	57
370	Nanovoid Formation and Annihilation in Gallium Nanodroplets under Lithiation–Delithiation Cycling. Nano Letters, 2013, 13, 5212-5217.	4.5	96
371	Shear responses of \$[ar{1},1,0]\$ -tilt {1 1 5}/{1 1 1} asymmetric tilt grain boundaries in fcc ma atomistic simulations. Modelling and Simulation in Materials Science and Engineering, 2013, 21, 055013.	etals by	14
372	In-Situ Transmission Electron Microscopy Observation of Solid Electrolyte Interface Formation On Si Nanowire Electrode in the Li-Ion Battery Using Liquid Confining Cell. ECS Meeting Abstracts, 2013, , .	0.0	0
373	"Conjugate Channeling―Effect in Dislocation Core Diffusion: Carbon Transport in Dislocated BCC Iron. PLoS ONE, 2013, 8, e60586.	1.1	26
374	Sample size effects on the large strain bursts in submicron aluminum pillars. Applied Physics Letters, 2012, 100, .	1.5	67
375	Patterning of graphene. Nanoscale, 2012, 4, 4883.	2.8	107
376	Quantitative Fracture Strength and Plasticity Measurements of Lithiated Silicon Nanowires by <i>In Situ</i> TEM Tensile Experiments. ACS Nano, 2012, 6, 9425-9432.	7.3	106
377	In situ atomic-scale imaging of electrochemical lithiation in silicon. Nature Nanotechnology, 2012, 7, 749-756.	15.6	533
378	Strain-engineered artificial atom as a broad-spectrum solar energy funnel. Nature Photonics, 2012, 6, 866-872.	15.6	907

#	Article	IF	CITATIONS
379	Icosahedral Platinum Alloy Nanocrystals with Enhanced Electrocatalytic Activities. Journal of the American Chemical Society, 2012, 134, 11880-11883.	6.6	496
380	A metamaterial with memory. Nature Nanotechnology, 2012, 7, 773-774.	15.6	8
381	Finding activation pathway of coupled displacive-diffusional defect processes in atomistics: Dislocation climb in fcc copper. Physical Review B, 2012, 86, .	1.1	25
382	Adaptive-boost molecular dynamics simulation of carbon diffusion in iron. Physical Review B, 2012, 85,	1.1	43
383	Breakup of spherical vesicles caused by spontaneous curvature change. Acta Mechanica Sinica/Lixue Xuebao, 2012, 28, 1545-1550.	1.5	2
384	Adsorbate interactions on surface lead to a flattened Sabatier volcano plot in reduction of oxygen. Journal of Catalysis, 2012, 295, 59-69.	3.1	24
385	Slip corona surrounding bilayer graphene nanopore. Nanoscale, 2012, 4, 5989.	2.8	12
386	Orientation-Dependent Interfacial Mobility Governs the Anisotropic Swelling in Lithiated Silicon Nanowires. Nano Letters, 2012, 12, 1953-1958.	4.5	212
387	Electrical Wind Force–Driven and Dislocation-Templated Amorphization in Phase-Change Nanowires. Science, 2012, 336, 1561-1566.	6.0	162
388	Hydrogen embrittlement of ferritic steels: Observations on deformation microstructure, nanoscale dimples and failure by nanovoiding. Acta Materialia, 2012, 60, 5160-5171.	3.8	274
389	Sample size matters for Al88Fe7Gd5 metallic glass: Smaller is stronger. Acta Materialia, 2012, 60, 5370-5379.	3.8	110
390	The Nanostructured Origin of Deformation Twinning. Nano Letters, 2012, 12, 887-892.	4.5	218
391	Simulations and generalized model of the effect of filler size dispersity on electrical percolation in rod networks. Physical Review B, 2012, 86, .	1.1	80
392	Approaching the ideal elastic limit of metallic glasses. Nature Communications, 2012, 3, 609.	5.8	345
393	Highly Active Pt ₃ Pb and Core–Shell Pt ₃ Pb–Pt Electrocatalysts for Formic Acid Oxidation. ACS Nano, 2012, 6, 2818-2825.	7.3	177
394	Strain-Engineering of Band Gaps in Piezoelectric Boron Nitride Nanoribbons. Nano Letters, 2012, 12, 1224-1228.	4.5	181
395	Ionomigration of Neutral Phases in Ionic Conductors. Advanced Energy Materials, 2012, 2, 1383-1389.	10.2	20
396	In Situ TEM Experiments of Electrochemical Lithiation and Delithiation of Individual Nanostructures. Advanced Energy Materials, 2012, 2, 722-741.	10.2	341

#	Article	IF	CITATIONS
397	Pristine-to-pristine regime of plastic deformation in submicron-sized single crystal gold particles. Acta Materialia, 2012, 60, 1368-1377.	3.8	33
398	In situ transmission electron microscopy of electrochemical lithiation, delithiation and deformation of individual graphene nanoribbons. Carbon, 2012, 50, 3836-3844.	5.4	98
399	The Possibility of Chemically Inert, Graphene-Based All-Carbon Electronic Devices with 0.8 eV Gap. ACS Nano, 2011, 5, 3475-3482.	7.3	49
400	Leapfrog Cracking and Nanoamorphization of ZnO Nanowires during In Situ Electrochemical Lithiation. Nano Letters, 2011, 11, 4535-4541.	4.5	169
401	Lithium fiber growth on the anode in a nanowire lithium ion battery during charging. Applied Physics Letters, 2011, 98, .	1.5	80
402	Anisotropic Swelling and Fracture of Silicon Nanowires during Lithiation. Nano Letters, 2011, 11, 3312-3318.	4.5	691
403	Lithiation-Induced Embrittlement of Multiwalled Carbon Nanotubes. ACS Nano, 2011, 5, 7245-7253.	7.3	122
404	Reversible Nanopore Formation in Ge Nanowires during Lithiation–Delithiation Cycling: An In Situ Transmission Electron Microscopy Study. Nano Letters, 2011, 11, 3991-3997.	4.5	356
405	Diffusive molecular dynamics and its application to nanoindentation and sintering. Physical Review B, 2011, 84, .	1.1	67
406	Time scale bridging in atomistic simulation of slow dynamics: viscous relaxation and defect activation. European Physical Journal B, 2011, 82, 271-293.	0.6	36
407	Emergence of strain-rate sensitivity in Cu nanopillars: Transition from dislocation multiplication to dislocation nucleation. Acta Materialia, 2011, 59, 5627-5637.	3.8	162
408	Modeling displacive–diffusional coupled dislocation shearing of γ′ precipitates in Ni-base superalloys. Acta Materialia, 2011, 59, 3484-3497.	3.8	57
409	A new regime for mechanical annealing and strong sample-size strengthening in body centred cubic molybdenum. Nature Communications, 2011, 2, 547.	5.8	84
410	Computing the Viscosity of Supercooled Liquids: Markov Network Model. PLoS ONE, 2011, 6, e17909.	1.1	28
411	In Situ Observation of the Electrochemical Lithiation of a Single SnO ₂ Nanowire Electrode. Science, 2010, 330, 1515-1520.	6.0	1,430
412	High-Efficiency Mechanical Energy Storage and Retrieval Using Interfaces in Nanowires. Nano Letters, 2010, 10, 1774-1779.	4.5	63
413	In situ imaging of layer-by-layer sublimation of suspended graphene. Nano Research, 2010, 3, 43-50.	5.8	40
414	Electrical Percolation Behavior in Silver Nanowire–Polystyrene Composites: Simulation and Experiment. Advanced Functional Materials, 2010, 20, 2709-2716.	7.8	173

#	Article	IF	CITATIONS
415	Ultra-strength materials. Progress in Materials Science, 2010, 55, 710-757.	16.0	696
416	Lattice dynamical finite-element method. Acta Materialia, 2010, 58, 510-523.	3.8	19
417	Phase field modeling of defects and deformation. Acta Materialia, 2010, 58, 1212-1235.	3.8	365
418	In situ observations of the nucleation and growth of atomically sharp graphene bilayer edges. Carbon, 2010, 48, 2354-2360.	5.4	33
419	Strong crystal size effect on deformation twinning. Nature, 2010, 463, 335-338.	13.7	553
420	Adaptive strain-boost hyperdynamics simulations of stress-driven atomic processes. Physical Review B, 2010, 82, .	1.1	66
421	Superelasticity in bcc nanowires by a reversible twinning mechanism. Physical Review B, 2010, 82, .	1.1	99
422	Inverse martensitic transformation in Zr nanowires. Physical Review B, 2010, 81, .	1.1	28
423	Screw dislocation mobility in BCC metals: the role of the compact core on double-kink nucleation. Modelling and Simulation in Materials Science and Engineering, 2010, 18, 085008.	0.8	80
424	Phase Diagrams for Multi-Component Membrane Vesicles: A Coarse-Grained Modeling Study. Langmuir, 2010, 26, 12659-12666.	1.6	19
425	Calculating phase-coherent quantum transport in nanoelectronics withab initioquasiatomic orbital basis set. Physical Review B, 2010, 82, .	1.1	16
426	One-particle-thick, solvent-free, coarse-grained model for biological and biomimetic fluid membranes. Physical Review E, 2010, 82, 011905.	0.8	106
427	Atomistic modeling of interfaces and their impact on microstructure and properties. Acta Materialia, 2010, 58, 1117-1151.	3.8	430
428	Double-inverse grain size dependence of deformation twinning in nanocrystalline Cu. Physical Review B, 2010, 81, .	1.1	88
429	Variable Nanoparticle-Cell Adhesion Strength Regulates Cellular Uptake. Physical Review Letters, 2010, 105, 138101.	2.9	166
430	Pressure-temperature phase diagram for shapes of vesicles: A coarse-grained molecular dynamics study. Applied Physics Letters, 2009, 95, 143104.	1.5	10
431	Toughness scale from first principles. Journal of Applied Physics, 2009, 106, .	1.1	38
432	In situ observation of graphene sublimation and multi-layer edge reconstructions. Proceedings of the National Academy of Sciences of the United States of America, 2009, 106, 10103-10108.	3.3	232

#	Article	IF	CITATIONS
433	Mechanics of Ultra-Strength Materials. MRS Bulletin, 2009, 34, 167-172.	1.7	105
434	Size dependence of rate-controlling deformation mechanisms in nanotwinned copper. Scripta Materialia, 2009, 60, 1062-1066.	2.6	88
435	Sizeâ€Dependent Endocytosis of Nanoparticles. Advanced Materials, 2009, 21, 419-424.	11.1	895
436	The intermediate temperature deformation of Ni-based superalloys: Importance of reordering. Jom, 2009, 61, 42-48.	0.9	41
437	Microtwinning and other shearing mechanisms at intermediate temperatures in Ni-based superalloys. Progress in Materials Science, 2009, 54, 839-873.	16.0	305
438	Computing the viscosity of supercooled liquids. Journal of Chemical Physics, 2009, 130, 224504.	1.2	128
439	Geometric and electronic structure of graphene bilayer edges. Physical Review B, 2009, 80, .	1.1	60
440	Computing the viscosity of supercooled liquids. II. Silica and strong-fragile crossover behavior. Journal of Chemical Physics, 2009, 131, 164505.	1.2	44
441	Atomistic Simulations of Dislocations in Confined Volumes. MRS Bulletin, 2009, 34, 184-189.	1.7	50
442	Finding Critical Nucleus in Solid-State Transformations. Metallurgical and Materials Transactions A: Physical Metallurgy and Materials Science, 2008, 39, 976-983.	1.1	46
443	Tight-binding Hamiltonian from first-principles calculations. Scientific Modeling and Simulation SMNS, 2008, 15, 81-95.	0.8	9
444	Atomistic simulation studies of complex carbon and silicon systems using environment-dependent tight-binding potentials. Scientific Modeling and Simulation SMNS, 2008, 15, 97-121.	0.8	4
445	Thermochemical and Mechanical Stabilities of the Oxide Scale of ZrB ₂ +SiC and Oxygen Transport Mechanisms. Journal of the American Ceramic Society, 2008, 91, 1475-1480.	1.9	83
446	Deformation of the ultra-strong. Nature, 2008, 456, 716-717.	13.7	71
447	Temperature and Strain-Rate Dependence of Surface Dislocation Nucleation. Physical Review Letters, 2008, 100, 025502.	2.9	587
448	Hydrostatic compression and high-pressure elastic constants of coesite silica. Journal of Applied Physics, 2008, 103, 053506.	1.1	23
449	Near Neutrality of an Oxygen Molecule Adsorbed on a Pt(111) Surface. Physical Review Letters, 2008, 101, 146101.	2.9	51
450	Quasiatomic orbitals for <i>ab initio</i> tight-binding analysis. Physical Review B, 2008, 78, .	1.1	90

#	Article	IF	CITATIONS
451	Atomistic simulation studies of complex carbon and silicon systems using environment-dependent tight-binding potentials. Lecture Notes in Computational Science and Engineering, 2008, , 97-121.	0.1	1
452	Plastic bending and shape-memory effect of double-wall carbon nanotubes. Physical Review B, 2007, 76,	1.1	21
453	Cytoskeletal dynamics of human erythrocyte. Proceedings of the National Academy of Sciences of the United States of America, 2007, 104, 4937-4942.	3.3	234
454	Complete set of elastic constants ofα-quartz at high pressure: A first-principles study. Physical Review B, 2007, 75, .	1.1	59
455	Mechanism of Thermal Transport in Dilute Nanocolloids. Physical Review Letters, 2007, 98, 028302.	2.9	136
456	Theory of Shear Banding in Metallic Glasses and Molecular Dynamics Calculations. Materials Transactions, 2007, 48, 2923-2927.	0.4	895
457	Multiscale Materials Modelling: Case Studies at the Atomistic and Electronic Structure Levels. ESAIM: Mathematical Modelling and Numerical Analysis, 2007, 41, 427-445.	0.8	3
458	The Mechanics and Physics of Defect Nucleation. MRS Bulletin, 2007, 32, 151-159.	1.7	139
459	<i>Ab initio</i> calculation of ideal strength and phonon instability of graphene under tension. Physical Review B, 2007, 76, .	1.1	1,225
460	Interfacial plasticity governs strain rate sensitivity and ductility in nanostructured metals. Proceedings of the National Academy of Sciences of the United States of America, 2007, 104, 3031-3036.	3.3	522
461	Ductile crystalline-amorphous nanolaminates. Proceedings of the National Academy of Sciences of the United States of America, 2007, 104, 11155-11160.	3.3	419
462	Deciding the Nature of the Coarse Equation through Microscopic Simulations: The Baby-Bathwater Scheme. SIAM Review, 2007, 49, 469-487.	4.2	39
463	Dynamical thermal conductivity of argon crystal. Journal of Applied Physics, 2007, 102, 043514.	1.1	47
464	Thermal expansion and atomic vibrations of zirconium carbide to 1600 K. Philosophical Magazine, 2007, 87, 2507-2519.	0.7	37
465	Highly localized quasiatomic minimal basis orbitals for Mo fromab initiocalculations. Physical Review B, 2007, 76, .	1.1	41
466	Beyond the Maxwell limit: Thermal conduction in nanofluids with percolating fluid structures. Physical Review E, 2007, 76, 062501.	0.8	67
467	Indentation across size scales and disciplines: Recent developments in experimentation and modeling. Acta Materialia, 2007, 55, 4015-4039.	3.8	403
468	Molecular dynamics study on the formation of stacking fault tetrahedra and unfaulting of Frank loops in fcc metals. Acta Materialia, 2007, 55, 3073-3080.	3.8	63

#	Article	IF	CITATIONS
469	Fast Mass Transport Through Carbon Nanotube Membranes. Small, 2007, 3, 1996-2004.	5.2	146
470	Nanomechanics of Crack Front Mobility. , 2006, , 217-223.		0
471	A Perspective on Modeling Materials in Extreme Environments: Oxidation of Ultrahigh-Temperature Ceramics. MRS Bulletin, 2006, 31, 410-418.	1.7	49
472	Theoretical assessment of the elastic constants and hydrogen storage capacity of some metal-organic framework materials. Journal of Chemical Physics, 2006, 125, 084714.	1.2	94
473	Atomistic characterization of three-dimensional lattice trapping barriers to brittle fracture. Proceedings of the Royal Society A: Mathematical, Physical and Engineering Sciences, 2006, 462, 1741-1761.	1.0	36
474	Atomistic simulation of the influence of pressure on dislocation nucleation in bcc Mo. Computational Materials Science, 2006, 36, 60-64.	1.4	15
475	Encoding electronic structure information in potentials for multi-scale simulations: SiO2. Computational Materials Science, 2006, 38, 340-349.	1.4	2
476	Atomistic simulation of shear localization in Cu–Zr bulk metallic glass. Intermetallics, 2006, 14, 1033-1037.	1.8	124
477	Yield point of metallic glass. Acta Materialia, 2006, 54, 4293-4298.	3.8	231
478	Molecularly based analysis of deformation of spectrin network and human erythrocyte. Materials Science and Engineering C, 2006, 26, 1232-1244.	3.8	190
479	Atomistic simulation of rapid compression of fractured silicon carbide. Journal of Nuclear Materials, 2006, 352, 22-28.	1.3	8
480	Spectral Method for Thermal Conductivity Calculations. Journal of Computer-Aided Materials Design, 2006, 12, 141-159.	0.7	7
481	Atomic Scale Chemo-mechanics of Silica: Nano-rod Deformation and Water Reaction. Journal of Computer-Aided Materials Design, 2006, 13, 135-159.	0.7	16
482	Coverage dependence and hydroperoxyl-mediated pathway of catalytic water formation on Pt (111) surface. Journal of Chemical Physics, 2006, 125, 054701.	1.2	61
483	Time-dependent density functional theory with ultrasoft pseudopotentials: Real-time electron propagation across a molecular junction. Physical Review B, 2006, 73, .	1.1	74
484	Energetics of plastic bending of carbon nanotubes. Physical Review B, 2006, 74, .	1.1	30
485	Undissociated screw dislocation in Si: Glide or shuffle set?. Applied Physics Letters, 2006, 89, 051910.	1.5	33
486	Multiple self-localized electronic states in trans-polyacetylene. Proceedings of the National Academy of Sciences of the United States of America, 2006, 103, 8943-8946.	3.3	21

#	Article	IF	CITATIONS
487	Stress-dependent molecular pathways of silica–water reaction. Journal of the Mechanics and Physics of Solids, 2005, 53, 1597-1623.	2.3	114
488	Near-surface lattice instability in 2D fiber and half-space. Acta Materialia, 2005, 53, 1215-1224.	3.8	43
489	Energy landscape of deformation twinning in bcc and fcc metals. Physical Review B, 2005, 71, .	1.1	215
490	Polaron-induced conformation change in single polypyrrole chain: An intrinsic actuation mechanism. International Journal of Quantum Chemistry, 2005, 102, 980-985.	1.0	52
491	Controlling Bending and Twisting of Conjugated Polymers via Solitons. Physical Review Letters, 2005, 95, 198303.	2.9	21
492	Theoretical strength of 2D hexagonal crystals: application to bubble raft indentation. Philosophical Magazine, 2005, 85, 2177-2195.	0.7	29
493	Statistical field estimators for multiscale simulations. Physical Review E, 2005, 72, 056712.	0.8	6
494	Spectrin-Level Modeling of the Cytoskeleton and Optical Tweezers Stretching of the Erythrocyte. Biophysical Journal, 2005, 88, 3707-3719.	0.2	376
495	Nanomechanics of Crack Front Mobility. Journal of Applied Mechanics, Transactions ASME, 2005, 72, 932-935.	1.1	3
496	Ab initiostudy of the surface properties and ideal strength of (100) silicon thin films. Physical Review B, 2005, 72, .	1.1	59
497	Basic Molecular Dynamics. , 2005, , 565-588.		24
498	Atomistic Calculation of Mechanical Behavior. , 2005, , 773-792.		1
499	Atomistic Visualization. , 2005, , 1051-1068.		9
500	Atomistic Visualization. , 2005, , 1051-1068.		1
501	Atomistic Calculation of Mechanical Behavior. , 2005, , 773-792.		0
502	Atomistic Configurations and Energetics of Crack Extension in Silicon. Physical Review Letters, 2004, 93, 205504.	2.9	58
503	Transformation strain by chemical disordering in silicon carbide. Journal of Applied Physics, 2004, 95, 6466-6469.	1.1	14
504	Breaking Atomic Bonds through Vibrational Mode Localization. Defect and Diffusion Forum, 2004, 233-234, 49-60.	0.4	2

#	Article	IF	CITATIONS
505	Analysis of shear deformations in Al and Cu: empirical potentials versus density functional theory. Modelling and Simulation in Materials Science and Engineering, 2004, 12, 1017-1029.	0.8	36
506	Twinning pathway in BCC molybdenum. Europhysics Letters, 2004, 68, 405-411.	0.7	26
507	Response to "Comment on †Theoretical evaluation of hydrogen storage capacity in pure carbon nanostructures' ―[J. Chem. Phys. 120, 9427 (2003)]. Journal of Chemical Physics, 2004, 120, 9430-9432	. 1.2	5
508	Ideal shear strain of metals and ceramics. Physical Review B, 2004, 70, .	1.1	334
509	Elastic criterion for dislocation nucleation. Materials Science & Engineering A: Structural Materials: Properties, Microstructure and Processing, 2004, 365, 25-30.	2.6	52
510	Dislocation slip or deformation twinning: confining pressure makes a difference. Materials Science & Engineering A: Structural Materials: Properties, Microstructure and Processing, 2004, 387-389, 840-844.	2.6	28
511	Predictive modeling of nanoindentation-induced homogeneous dislocation nucleation in copper. Journal of the Mechanics and Physics of Solids, 2004, 52, 691-724.	2.3	227
512	Dislocation Core Effects on Mobility. Dislocations in Solids, 2004, 12, 1-80.	1.6	120
513	Core energy and Peierls stress of a screw dislocation in bcc molybdenum: A periodic-cell tight-binding study. Physical Review B, 2004, 70, .	1.1	105
514	Atomistic Study of Dislocation Loop Emission from a Crack Tip. Physical Review Letters, 2004, 93, 025503.	2.9	192
515	Ab Initio Study of Ideal Shear Strength. Solid Mechanics and Its Applications, 2004, , 401-410.	0.1	4
516	Multiscale Modeling of Defect Nucleation and Reaction: Bulk to Nanostructures. Solid Mechanics and Its Applications, 2004, , 223-233.	0.1	1
517	Nonlinear Dynamics Analysis through Molecular Dynamics Simulations. Lecture Notes in Computational Science and Engineering, 2004, , 69-79.	0.1	0
518	Defect Nucleation. Solid Mechanics and Its Applications, 2004, , 203-211.	0.1	0
519	Crack-tip dislocation nanostructures in dynamical fracture of fcc metals: A molecular dynamics study. Journal of Computer-Aided Materials Design, 2003, 10, 143-154.	0.7	22
520	The gap-tooth method in particle simulations. Physics Letters, Section A: General, Atomic and Solid State Physics, 2003, 316, 190-195.	0.9	94
521	Atomistic modeling of mechanical behavior. Acta Materialia, 2003, 51, 5711-5742.	3.8	115
522	Force-based many-body interatomic potential for ZrC. Journal of Applied Physics, 2003, 93, 9072-9085.	1.1	49

#	Article	IF	CITATIONS
523	Computer Modeling Study of the Effect of Hydration on the Stability of a Silica Nanotube. Nano Letters, 2003, 3, 1347-1352.	4.5	53
524	Periodic image effects in dislocation modelling. Philosophical Magazine, 2003, 83, 539-567.	0.7	185
525	Deciding the Nature of the Coarse Equation through Microscopic Simulations: The Baby-Bathwater Scheme. Multiscale Modeling and Simulation, 2003, 1, 391-407.	0.6	26
526	AtomEye: an efficient atomistic configuration viewer. Modelling and Simulation in Materials Science and Engineering, 2003, 11, 173-177.	0.8	1,083
527	Theoretical evaluation of hydrogen storage capacity in pure carbon nanostructures. Journal of Chemical Physics, 2003, 119, 2376-2385.	1.2	263
528	Quantifying the early stages of plasticity through nanoscale experiments and simulations. Physical Review B, 2003, 67, .	1.1	361
529	Size effects on the onset of plastic deformation during nanoindentation of thin films and patterned lines. Journal of Applied Physics, 2003, 94, 6050-6058.	1.1	94
530	Deformation and Fracture of a SiO2Nanorod. Molecular Simulation, 2003, 29, 671-676.	0.9	36
531	Simulation of nanoindentation via interatomic potential finite element method. , 2003, , 795-799.		1
532	Ideal Pure Shear Strength of Aluminum and Copper. Science, 2002, 298, 807-811.	6.0	686
533	Atomistic mechanisms governing elastic limit and incipient plasticity in crystals. Nature, 2002, 418, 307-310.	13.7	621
534	Atomistic simulation of matter under stress: crossover from hard to soft materials. Physica A: Statistical Mechanics and Its Applications, 2002, 304, 11-22.	1.2	9
535	Mechanistic aspects and atomic-level consequences of elastic instabilities in homogeneous crystals. Materials Science & Engineering A: Structural Materials: Properties, Microstructure and Processing, 2001, 317, 236-240.	2.6	123
536	Anisotropic Elastic Interactions of a Periodic Dislocation Array. Physical Review Letters, 2001, 86, 5727-5730.	2.9	102
537	Atomistic measures of mechanical deformation and thermal transport processes. , 2001, , 1430-1433.		0
538	Optimal particle controller for coupled continuum/MD fluid simulation. , 2001, , 895-898.		0
539	Nearly exact solution for coupled continuum/MD fluid simulation. Journal of Computer-Aided Materials Design, 1999, 6, 95-102.	0.7	34
540	Atomistic modeling of finite-temperature properties of crystalline β-SiC. Journal of Nuclear Materials, 1998, 255, 139-152.	1.3	244

#	Article	IF	CITATIONS
541	Thermal Conductivity of Solid Argon by Classical Molecular Dynamics. Materials Research Society Symposia Proceedings, 1998, 538, 503.	0.1	31
542	Coupling continuum to molecular-dynamics simulation: Reflecting particle method and the field estimator. Physical Review E, 1998, 57, 7259-7267.	0.8	119
543	Imposing Field Boundary Conditions in MD Simulation of Fluids: Optimal Particle Controller and Buffer Zone Feedback. Materials Research Society Symposia Proceedings, 1998, 538, 473.	0.1	15
544	Order-Nmethod to calculate the local density of states. Physical Review B, 1997, 56, 3524-3527.	1.1	16
545	Atomistic modeling of finite-temperature properties of β-SiC. I. Lattice vibrations, heat capacity, and thermal expansion. Journal of Nuclear Materials, 1997, 246, 53-59.	1.3	89
546	Unifying two criteria of Born: Elastic instability and melting of homogeneous crystals. Physica A: Statistical Mechanics and Its Applications, 1997, 240, 396-403.	1.2	70
547	Mechanical instabilities of homogeneous crystals. Physical Review B, 1995, 52, 12627-12635.	1.1	432